Thermodynamics of two-dimensional ideal ferromagnets: Three-loop analysis

Christoph P. Hofmann[*]

Facultad de Ciencias, Universidad de Colima, Bernal Díaz del Castillo 340, Colima, C.P. 28045, Mexico

Within the effective Lagrangian framework, we explicitly evaluate the partition function of two-dimensional ideal ferromagnets up to three loops at low temperatures and in the presence of a weak external magnetic field. The low-temperature series for the free energy density, energy density, heat capacity, entropy density, and magnetization are given and their range of validity is critically examined in view of the Mermin-Wagner theorem. The calculation involves the renormalization and numerical evaluation of a particular three-loop graph, which is discussed in detail. Interestingly, in the low-temperature series for the two-dimensional ideal ferromagnet, the spin-wave interaction manifests itself in the form of logarithmic terms. In the free energy density the leading such term is of order $T^4 \ln T$: remarkably, in the case of the three-dimensional ideal ferromagnet no logarithmic terms arise in the low-temperature series. While the present study demonstrates that it is straightforward to consider effects up to three-loop order in the effective field theory framework, this precision seems to be far beyond the reach of microscopic methods such as spin-wave theory.

I. INTRODUCTION

In a very recent article on the thermodynamic properties of two-dimensional ideal ferromagnets,[1] the general structure of the low-temperature series for the free energy density has been discussed using the method of effective Lagrangians. In particular, it has been argued that the spin-wave interaction does not yet manifest itself at order T^3 in the free energy density; it only shows up at order $T^4 \ln T$. The explicit evaluation of the various Feynman graphs contributing at this order, however, has not been performed in that reference; this is the subject of the present article. The calculation involves a particular three-loop graph whose renormalization and subsequent numerical evaluation—although quite elaborate— is rather straightforward within the effective field theory framework. While Ref. [1] focused on the low-temperature series for the free energy density, here we also consider the magnetization and critically examine the range of validity of the corresponding low-temperature series; indeed, in view of the Mermin-Wagner theorem, one has to be very careful by taking the limit of a zero external magnetic field H.

Interestingly, these logarithmic contributions $T^n \ln T$ in the partition function are restricted to two-dimensional ferromagnets and do not show up in the case of three-dimensional ideal ferromagnets. There the low-temperature series of the various thermodynamic quantities consist of integer and half-integer powers of the temperature.[2–5] Actually, the occurrence of such logarithmic contributions is well known in the domain of particle physics; the low-temperature expansion of, e.g., the free energy density in quantum chromodynamics also involves the logarithmic term $T^8 \ln T$ (see Ref. [6]). The term $T^8 \ln T$ also occurs in the low-temperature expansion of the free energy density of the three-dimensional antiferromagnet,[7] which obeys a linear, i.e., relativistic, dispersion law. Furthermore, logarithmic contributions in temperature expansions of thermodynamic quantities also occur in the context of one-dimensional condensed matter systems, such as in antiferromagnetic spin chains.[8–13]

We also examine our series obtained within the effective Lagrangian framework with the relevant literature and point out that our approach is much more efficient than conventional condensed matter methods such as spin-wave theory or Schwinger-Boson mean field theory. In particular, while all these different studies were restricted to the idealized picture of the free magnon gas, in the present article we discuss in detail how the spin-wave interaction manifests itself in the low-temperature behavior of the two-dimensional ideal ferromagnet.

The rest of the paper is organized as follows. In Sec. II we briefly discuss some essential aspects of the effective Lagrangian method; detailed accounts can be found in the references provided below. The evaluation of the partition function up to three-loop order in the low-temperature expansion is presented in Sec. III. While the renormalization up to order $p^6 \propto T^3$ turns out to be straightforward, the handling of ultraviolet divergences at order p^8 is more involved and is considered in detail in Sec. IV. The low-temperature expansions for the free energy density, energy density, heat capacity, and entropy density of the two-dimensional ideal ferromagnet are given in Sec. V. The low-temperature series for the magnetization is discussed in Sec. VI and the range of validity of this series is critically examined in view of the Mermin-Wagner theorem. Here we also compare our results with the condensed matter literature. While our conclusions are presented in Sec. VII, the numerical evaluation of a specific three-loop graph, the logarithmic renormalization of effective constants, the representation of the pressure at zero magnetic field, and the explicit low-temperature series are relegated to four separate Appendices.

Unfortunately, the systematic and model-independent effective Lagrangian method is still not very well known within the condensed matter community. Therefore we would like to provide the reader with a brief list of references in which condensed matter problems have been successfully solved within the effective field theory framework. These include antiferromagnets and ferromagnets in two and three spatial dimensions,[4,5,7,14–25] as well as two-dimensional antiferromagnets which are the precursors of high-temperature superconductors.[26–35]

Many different tests—both analytical and numerical studies—unambiguously confirm that the effective Lagrangian technique represents a rigorous and systematic framework to address condensed matter systems which exhibit a spontaneously broken symmetry. On the one hand, the correctness of the effective Lagrangian approach was demonstrated explicitly in Ref. 36 by comparing the microscopic results of an analytically solvable model for a hole-doped ferromagnet in $1 + 1$ dimensions with the effective theory predictions. On the other hand, in a series of high-accuracy investigations of the antiferromagnetic spin-$\frac{1}{2}$ quantum Heisenberg model on a square lattice using the loop-cluster algorithm,[37–40] the Monte Carlo data were confronted with the analytic predictions of the effective Lagrangian theory and the low-energy constants were extracted with per mille accuracy.

II. ESSENTIAL ASPECTS OF EFFECTIVE LAGRANGIANS

The present article deals with the explicit evaluation of the partition function of the two-dimensional ideal ferromagnet at three-loop order and the subsequent discussion of various thermodynamic quantities—including the magnetization—at low temperatures. It is an extension of the work presented in a recent article,[1] where the evaluation was restricted to two-loop order. The basic principles of the effective Lagrangian method and the perturbative evaluation of the partition function are outlined in Sec. II of that reference and are not repeated here in detail. The interested reader may also find a detailed account of finite-temperature effective Lagrangians in Appendix A in Ref. 5 and in the various references given therein. In addition, for pedagogic introductions to the effective Lagrangian technique, we refer to Refs. 41–45. In this section, we just focus on some essential aspects of the effective Lagrangian method at finite temperature.

The effective Lagrangian or, more precisely, the effective action

$$\mathcal{S}_{\text{eff}} = \int d^3 x \, \mathcal{L}_{\text{eff}} \tag{2.1}$$

of the two-dimensional ideal ferromagnet must share all the symmetries of the underlying Heisenberg model, i.e., the spontaneously broken spin rotation symmetry O(3), parity, and time reversal. The basic degrees of freedom of the effective Lagrangian are the two real magnon fields—or the physical magnon particle—which emerge due to the spontaneously broken spin symmetry O(3) → O(2).

A conceptual remark is in order here. On the microscopic level, the magnetic field $\vec{H}$ explicitly breaks the symmetry O(3) of the Heisenberg Hamiltonian down to O(2),

$$\mathcal{H} = -J \sum_{\text{n.n.}} \vec{S}_m \cdot \vec{S}_n - \mu \sum_n \vec{S}_n \cdot \vec{H}, \quad J = \text{const.} \tag{2.2}$$

In particle physics, such a situation is referred to as an *approximate* spontaneously broken symmetry, as opposed to an *exact* spontaneously broken symmetry. Using this language, the spontaneously broken symmetry O(3), due to the magnetic field, no longer is exact, but only approximate, and the Goldstone bosons turn into pseudo-Goldstone bosons, as they are now characterized by an energy gap. This is the situation

we are considering in the present study: the magnetic field is different from 0.

But a subtlety arises. Although the underlying Hamiltonian, (2.2), is only invariant under O(2), the effective action, (2.1), is still invariant under O(3). The detailed justification can be found in the pioneering article.[17] Here we just mention that this is because in the effective field theory framework, the global symmetry O(3) is promoted to a local one, in order to be able to account for the Ward identities, which reflect the symmetry properties of the theory on a local level. In particular, in that formalism, called the external field technique, the effective action, (2.1), is invariant under local O(3) transformations.

The various pieces in the effective Lagrangian are organized according to the number of space and time derivatives which act on the magnon fields. This derivative expansion—or expansion in powers of momentum—is completely systematic: At low energies, terms in the effective Lagrangian which contain only a few derivatives are the dominant ones, while terms with more derivatives are suppressed.[46–48] The leading-order effective Lagrangian for the ideal ferromagnet is of momentum order p^2 and takes the form[17]

$$\mathcal{L}_{\text{eff}}^2 = \Sigma \frac{\epsilon_{ab} \partial_0 U^a U^b}{1 + U^3} + \Sigma \mu H U^3 - \frac{1}{2} F^2 \partial_r U^i \partial_r U^i. \tag{2.3}$$

The two real components of the magnon field, $U^a (a = 1,2)$, are the first two components of the three-dimensional unit vector $U^i = (U^a, U^3)$. The quantity H is the third component of the magnetic field $\vec{H} = (0,0,H)$. While the derivative structure of the above terms is unambiguously determined by the symmetries of the underlying theory, the two *a priori* unknown low-energy constants—the spontaneous magnetization at zero temperature Σ and the constant F—have to be determined by experiment, numerical simulation, or comparison with the microscopic theory. Note that one time derivative (∂_0) is on the same footing as two space derivatives ($\partial_r \partial_r$), i.e., two powers of momentum count as only one power of energy or temperature: $k^2 \propto \omega, T$.

The next-to-leading-order Lagrangian for the ideal ferromagnet is of order p^4 and amounts to[4]

$$\mathcal{L}_{\text{eff}}^4 = l_1 (\partial_r U^i \partial_r U^i)^2 + l_2 (\partial_r U^i \partial_s U^i)^2 + l_3 \Delta U^i \Delta U^i, \tag{2.4}$$

where Δ denotes the Laplace operator in two spatial dimensions, $d_s = 2$, and the quantities l_1, l_2, and l_3 are effective coupling constants.

A crucial point underlying the perturbative evaluation of the partition function concerns the suppression of loop diagrams in the effective field theory framework. In two spatial dimensions, ferromagnetic loops are suppressed by two powers of momentum. This suppression rule lies at the heart of the organization of the Feynman graphs of the partition function for the two-dimensional ferromagnet depicted in Fig. 1. For example, the two-loop diagram 8d with an insertion from $\mathcal{L}_{\text{eff}}^4$, containing four magnon fields, is of order p^8, as it involves $\mathcal{L}_{\text{eff}}^4$ (p^4) and two loops (p^4).

An inspection of the diagrams in Fig. 1 reveals that insertions from $\mathcal{L}_{\text{eff}}^6$ only appear in the one-loop graph 8g. The only term we need for the present evaluation is thus quadratic
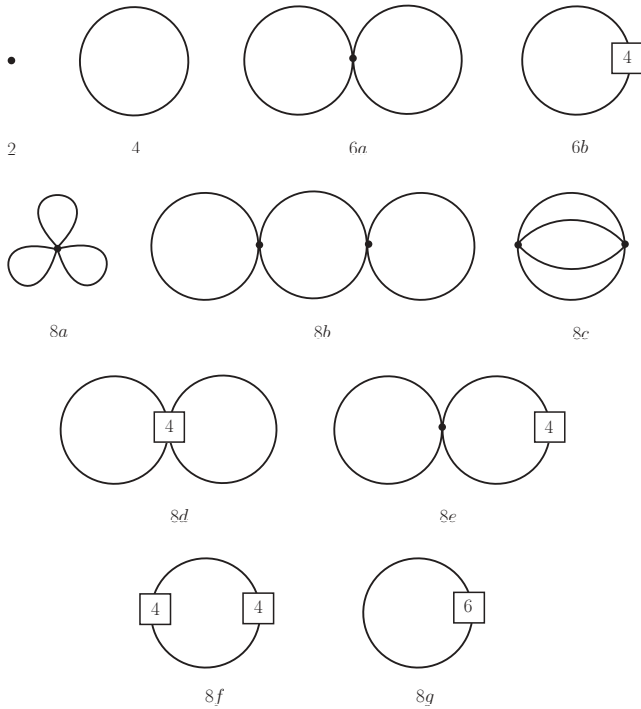
FIG. 1. Feynman graphs related to the low-temperature expansion of the partition function for a two-dimensional ferromagnet up to order p^8. The numbers attached to the vertices refer to the piece of the effective Lagrangian they come from. Vertices associated with the leading term $\mathcal{L}_{\text{eff}}^2$ are denoted by a filled circle. Note that ferromagnetic loops are suppressed by two powers of momentum in two spatial dimensions, $d_s = 2$.

in the magnon field,

$$\mathcal{L}_{\text{eff}}^6 = c_1 U^i \Delta^3 U^i, \tag{2.5}$$

where c_1 is an additional effective low-energy constant.

Lattice anisotropies do not yet manifest themselves in the leading-order effective Lagrangian $\mathcal{L}_{\text{eff}}^2$; expression (2.3) is invariant under continuous space rotations, even though the underlying lattices (square, honeycomb, triangular, and Kagomé, to name the most prominent ones) are only invariant under discrete space rotations. Although this accidental symmetry is restricted to $\mathcal{L}_{\text{eff}}^2$, in the present analysis we assume that the higher-order pieces $\mathcal{L}_{\text{eff}}^4$ and $\mathcal{L}_{\text{eff}}^6$ are O(3) space rotation invariant as well. The conclusions of the present paper are not affected by this idealization.

III. PARTITION FUNCTION UP TO THREE LOOPS

While the evaluation of the partition function of the two-dimensional ideal ferromagnet up to order p^6 was presented in Ref. 1, here we go one step farther and consider the evaluation up to order p^8, where three-loop graphs start to appear. This calculation is rather involved due to the renormalization and numerical evaluation of the three-loop graph 8c.

As depicted in Fig. 1, there are only four Feynman diagrams that contribute to the partition function up to order p^6 or, equivalently, up to order T^3. The evaluation of these diagrams can be found in Ref. 1; the final expression for the free energy

density amounts to

$$z = -\Sigma \mu H - \frac{1}{4\pi\gamma} T^2 \sum_{n=1}^{\infty} \frac{e^{-\mu H n \beta}}{n^2}$$
$$- \frac{l_3}{\pi \Sigma \gamma^3} T^3 \sum_{n=1}^{\infty} \frac{e^{-\mu H n \beta}}{n^3} + \mathcal{O}(p^8), \tag{3.1}$$

where $\beta \equiv 1/T$ and H is the external magnetic field. The terms of order T^2 and T^3 arise from one-loop graphs and thus represent contributions to the free energy density originating from noninteracting spin waves. While the former term is exclusively determined by the leading-order effective constants Σ and F ($\gamma = F^2/\Sigma$), the term of order T^3, on the other hand, involves the next-to-leading-order effective constant l_3 from $\mathcal{L}_{\text{eff}}^4$. What is quite remarkable is that the spin-wave interaction does not yet manifest itself at this order in the low-temperature expansion of the free energy density. The only potential candidate, the two-loop diagram 6a of order T^3, turns out to be 0 due to parity.[1]

Before we evaluate the partition function at order p^8, we have to recall that, at finite temperature, the propagator is given by

$$G(x) = \sum_{n=-\infty}^{\infty} \Delta(\vec{x}, x_4 + n\beta), \tag{3.2}$$

where $\Delta(x)$ is the Euclidean propagator of ferromagnetic magnons at zero temperature,

$$\Delta(x) = \int \frac{dk_4 d^2 k}{(2\pi)^3} \frac{e^{i\vec{k}\vec{x} - i k_4 x_4}}{\gamma \vec{k}^2 - i k_4 + \mu H}. \tag{3.3}$$

Let us stress the fact that it is advantageous here to work within the real-space imaginary-time representation for the propagators, rather than within the momentum-frequency representation. This will become more evident in Sec. IV, where we analyze the ultraviolet divergences that occur in the limit $x \to 0$ in terms of Taylor expansions around that limit and perform the renormalization at the three-loop level.

For other condensed matter applications it would be more convenient to use the momentum-frequency representation for the propagators. The discrete sums in the imaginary time coordinate then show up as Matsubara frequencies. The connection between the two representations is given by a Fourier transform, the thermal Matsubara propagator $\mathcal{G}(\vec{k}, \omega + 2\pi n/\beta)$ in two spatial dimensions given by

$$\mathcal{G}(\vec{k}, \omega_n) = \int_0^\beta dx_4 \int d^2 x \, e^{i\omega_n x_4 - i\vec{k}\vec{x}} \Delta(\vec{x}, x_4), \tag{3.4}$$

with

$$\omega_n = 2\pi n/\beta. \tag{3.5}$$

An explicit representation for the thermal propagator $G(x)$, dimensionally regularized in the spatial dimension d_s, is

$$G(x) = \frac{1}{(4\pi\gamma)^{\frac{d_s}{2}}} \sum_{n=-\infty}^{\infty} \frac{1}{x_n^{\frac{d_s}{2}}} e^{-\frac{\vec{x}^2}{4\gamma x_n} - \mu H x_n} \Theta(x_n), \tag{3.6}$$

with

$$x_n \equiv x_4 + n\beta. \tag{3.7}$$

Also, it is convenient to introduce the notation,

$$G_1 \equiv [G(x)]_{x=0}, \quad G_\Delta \equiv [\Delta G(x)]_{x=0},$$
$$G_{\Delta^n} \equiv [\Delta^n G(x)]_{x=0}, \tag{3.8}$$

where Δ represents the Laplace operator in the spatial dimensions; note that the quantity $\Delta(x)$, on the other hand, stands for the zero-temperature propagator.

The quantities G_1 and G_Δ, as well as thermal propagators involving even higher-order space derivatives, can be split into a finite piece, which is temperature dependent, and a divergent piece, which is temperature independent:

$$G_1 = G_1^T + G_1^0, \quad G_\Delta = G_\Delta^T + G_\Delta^0. \tag{3.9}$$

The explicit dimensionally regularized expressions are

$$G_1^T = \frac{1}{(4\pi\gamma)^{\frac{d_s}{2}}} \sum_{n=1}^{\infty} \frac{e^{-\mu H n\beta}}{(n\beta)^{\frac{d_s}{2}}},$$
$$G_1^0 = \frac{1}{(4\pi\gamma)^{\frac{d_s}{2}}} \left[\frac{1}{x_4^{\frac{d_s}{2}}} e^{-\frac{\vec{x}^2}{4\gamma x_4}} \Theta(x_4) \right]_{x=0}, \tag{3.10}$$

and

$$G_\Delta^T = \frac{1}{(4\pi\gamma)^{\frac{d_s}{2}}} \left(-\frac{d_s}{2\gamma} \right) \sum_{n=1}^{\infty} \frac{e^{-\mu H n\beta}}{(n\beta)^{\frac{d_s}{2}+1}},$$
$$G_\Delta^0 = \frac{1}{(4\pi\gamma)^{\frac{d_s}{2}}} \left[\frac{1}{x_4^{\frac{d_s}{2}+1}} \left\{ \frac{-d_s}{2\gamma} + \frac{\vec{x}^2}{4\gamma^2 x_4} \right\} \right.$$
$$\left. \times \exp\left(-\frac{\vec{x}^2}{4\gamma x_4} \right) \Theta(x_4) \right]_{x=0}. \tag{3.11}$$

The temperature-independent pieces $G_1^0, G_\Delta^0, \ldots$ can be cast in the form

$$\frac{\exp[-x_4 \mu H]}{(\gamma x_4)^{m+\frac{d_s}{2}}} \Gamma\left(m + \frac{d_s}{2} \right), \quad m = 0,1,2,\ldots, \tag{3.12}$$

and rewritten as integrals over momentum,

$$\int d^{d_s} k(\vec{k}^2)^m \exp[-\gamma x_4 \vec{k}^2 - x_4 \mu H]\Theta(x_4). \tag{3.13}$$

In the limit $x_4 \to 0$ we are interested in, we are thus left with integrals over a polynomial. Now in dimensional regularization such expressions vanish altogether. The explicit proof can be found, e.g., in Ref. 62 [see formula (4.24b) there]. We thus conclude that the quantities G_1^0, G_Δ^0, and zero-temperature propagators involving higher order space derivatives do not contribute in the limit $d_s \to 2$. The only contributions we are thus left with here are those which involve the temperature-dependent pieces.

We add a remark regarding regularization. Within the context of effective Lagrangians it is most natural to use dimensional regularization, since in this scheme the symmetries of the theory are preserved. In the renormalization process, as we discuss in detail in Sec. IV and in Appendix B, the ultraviolet divergences occurring here can be absorbed into next-to-leading-order coupling constants, and most importantly, the resulting final expressions for the physical quantities do not depend on the renormalization scale $\tilde{\mu}$ (see Appendix B).

In the underlying theory, on the other hand, a more natural regularization for Heisenberg ferromagnets is the lattice

regularization, where ultraviolet divergences are absent. Still, a systematic three-loop calculation within the microscopic framework—the analog of the calculation presented here using effective field theory—seems to be presently out of sight. Note that spin-wave theory, Schwinger-boson mean field theory, and Green's function approaches make use of *ad hoc* assumptions or approximations and thus cannot be considered fully systematic.

According to Fig. 1, there are seven diagrams at order p^8 we need to evaluate. We first consider the two one-loop graphs which contain vertices from $\mathcal{L}_{\text{eff}}^4$ and $\mathcal{L}_{\text{eff}}^6$. For graph 8*g*, which only involves an insertion from $\mathcal{L}_{\text{eff}}^6$, we obtain

$$z_{8g} = -\frac{2c_1}{\Sigma} G_{\Delta^3}, \tag{3.14}$$

yielding the temperature-dependent contribution

$$z_{8g}^T = \frac{3c_1}{\pi\Sigma\gamma^4} T^4 \sum_{n=1}^{\infty} \frac{e^{-\mu H n\beta}}{n^4}. \tag{3.15}$$

Graph 8*f*, which contains two insertions from $\mathcal{L}_{\text{eff}}^4$, is proportional to an integral over the torus $\mathcal{T} = \mathcal{R}^{d_s} \times S^1$, with circle S^1 defined by $-\beta/2 \leqslant x_4 \leqslant \beta/2$, and involves a product of two thermal propagators,

$$z_{8f} = -\frac{2l_3^2}{\Sigma^2} \int_{\mathcal{T}} d^{d_s+1}x \, \Delta^2 G(x) \Delta^2 G(-x). \tag{3.16}$$

Integrals of this type, as shown in Ref. 4, can be converted into an expression displaying one propagator only,

$$-\int_{\mathcal{T}} d^{d_s+1}y \, \Delta^m G(-y) \Delta^n G(y) = \left[\Delta^{(m+n)} \frac{\partial G(x)}{\partial(\mu H)} \right]_{x=0}, \tag{3.17}$$

such that one ends up with

$$z_{8f} = \frac{2l_3^2}{\Sigma^2} \left[\Delta^4 \frac{\partial G(x)}{\partial(\mu H)} \right]_{x=0}. \tag{3.18}$$

Accordingly, the temperature-dependent part of graph 8f amounts to

$$z_{8f}^T = -\frac{12l_3^2}{\pi\Sigma^2\gamma^5} T^4 \sum_{n=1}^{\infty} \frac{e^{-\mu H n\beta}}{n^4}. \tag{3.19}$$

We now turn to the two-loop graphs which involve insertions from $\mathcal{L}_{\text{eff}}^2$ and $\mathcal{L}_{\text{eff}}^4$. Graph 8*d* contributes with

$$z_{8d} = -\frac{2}{3\Sigma^2}(8l_1 + 6l_2 + 5l_3)G_\Delta G_\Delta - \frac{2l_3}{\Sigma^2} G_1 G_{\Delta^2}. \tag{3.20}$$

The evaluation of graph 8*e* yields

$$z_{8e} = \frac{2l_3}{\Sigma^2} G_1 G_{\Delta^2}, \tag{3.21}$$

and cancels the second term in z_{8d}. For the temperature-dependent part originating from the two-loop graphs of order p^8, we thus end up with

$$z_{8[de]}^T = -\frac{8l_1 + 6l_2 + 5l_3}{24\pi^2\Sigma^2\gamma^4} T^4 \left\{ \sum_{n=1}^{\infty} \frac{e^{-\mu H n\beta}}{n^2} \right\}^2. \tag{3.22}$$

Finally, we consider the three-loop graphs. Note that they exclusively contain vertices from the leading-order Lagrangian $\mathcal{L}_{\text{eff}}^2$. Graph 8a factorizes into a product of three thermal propagators (and space derivatives thereof), to be evaluated at the origin:

$$z_{8a} = -\frac{F^2}{\Sigma^3} G_\Delta (G_1)^2. \qquad (3.23)$$

Remarkably, the three-loop graph 8b turns out to be 0,

$$z_{8b} = 0. \qquad (3.24)$$

Much like the two-loop graph 6a, the three-loop graph 8b does not contribute to the partition function.

We are left with the cateye graph 8c, which leads to

$$z_{8c} = -\frac{F^4}{2\Sigma^4} K + \frac{F^2}{\Sigma^3} G_\Delta (G_1)^2. \qquad (3.25)$$

The quantity K denotes the following integral over the torus involving a product of four thermal propagators:

$$K = \int_{\mathcal{T}} d^{d_s+1} x \, \partial_r G \partial_r G \partial_s \tilde{G} \partial_s \tilde{G}. \qquad (3.26)$$

Here we have used the notation

$$G = G(x), \quad \tilde{G} = G(-x). \qquad (3.27)$$

The second term in Eq. (3.25) cancels the contribution from graph 8a; hence the overall contribution from the three-loop graphs is just the one proportional to the integral K. Note that, unlike all other pieces in the free energy density up to order p^8, this quantity is not a product of thermal propagators (or derivatives thereof) to be evaluated at the origin; its structure is much more complicated. In the next section, as well as in Appendices A and B, we address in detail the renormalization and numerical evaluation of this integral, which contains a total of four infinite sums.

IV. RENORMALIZATION OF THE CATEYE GRAPH

Regarding the renormalization of the three-loop graph 8c, we follow the method outlined in Ref. 6, where the same graph was considered in a Lorentz-invariant framework. In order to isolate the ultraviolet divergences and to perform the renormalization, it is essential that we work here within the real-space imaginary-time representation for the propagators, rather than within the momentum-frequency representation.

The relevant integral from the three-loop contribution is given by

$$K = \int_{\mathcal{T}} d^{d_s+1} x \, \partial_r G \partial_r G \partial_s \tilde{G} \partial_s \tilde{G}$$

and involves a product of four thermal propagators. In order to analyze the limit $d_s \to 2$, the thermal propagators are split into two pieces:

$$G(x) = G^T(x) + \Delta(x). \qquad (4.1)$$

While the zero-temperature propagator $\Delta(x)$ contains the ultraviolet singularities, the temperature-dependent part $G^T(x)$ is finite as $d_s \to 2$. Note that, if we restrict ourselves to the origin, we reproduce the first relation in Eq. (3.9).

With the above decomposition, the integral K yields nine terms that can be grouped into the following six classes. For simplicity we do not display the derivatives.

$$
\begin{aligned}
\text{A}: \ & G^T(x)G^T(x)G^T(-x)G^T(-x), \\
\text{B}: \ & \Delta(x)G^T(x)G^T(-x)G^T(-x), \\
& G^T(x)G^T(x)\Delta(-x)G^T(-x), \\
\text{C}: \ & \Delta^2(x)G^T(-x)G^T(-x), \quad G^T(x)G^T(x)\Delta^2(-x), \\
\text{D}: \ & \Delta(x)G^T(x)\Delta(-x)G^T(-x), \\
\text{E}: \ & \Delta^2(x)\Delta(-x)G^T(-x), \quad \Delta(x)G^T(x)\Delta^2(-x), \\
\text{F}: \ & \Delta^2(x)\Delta^2(-x).
\end{aligned}
\qquad (4.2)
$$

As the product $\Delta(x)\Delta(-x)$ of zero-temperature propagators involves the combination $\Theta(x_4)\Theta(-x_4)$, terms of classes D, E, and F vanish identically. The maximum number of Θ functions a given term can contain—- in order not to be 0—is two. Also, the arguments of the two Θ functions have to coincide as is the case with the terms of class C. We conclude that we only have to consider cases A, B, and C.

Contributions from classes A and B are related to integrals over the torus,

$$\int_{\mathcal{T}} d^{d_s+1} x (\partial_r G^T \partial_r G^T \partial_s \tilde{G}^T \partial_s \tilde{G}^T + 4\partial_r \Delta \partial_r G^T \partial_s \tilde{G}^T \partial_s \tilde{G}^T), \qquad (4.3)$$

which are not singular at $d_s = 2$.

Terms of class C, on the other hand, do lead to an ultraviolet-divergent integral. Consider, e.g., the term

$$\partial_r \Delta(x) \partial_r \Delta(x) \partial_s G^T(-x) \partial_s G^T(-x), \qquad (4.4)$$

where we now have included the derivatives. In the limit $d_s \to 2$, the zero-temperature piece $\partial_r \Delta(x)$ amounts to

$$\partial_r \Delta(x) \propto \frac{x^r}{x_4^2} \exp\left[-\frac{\vec{x}^2}{4\gamma x_4} \right]. \qquad (4.5)$$

The Taylor series of the function $\partial_s G^T(-x)$, evaluated at the origin, starts with a term linear in $\vec{x}$:

$$\partial_s G^T(-x) = \partial_{\alpha s} G^T(-x)|_{x=0} x^\alpha + \mathcal{O}(\vec{x}^3). \qquad (4.6)$$

Inserting this term into Eq. (4.4), in the limit $d_s \to 2$, we end up with the following contribution in K,

$$K \propto \int d^2 x \, dx_4 \left(\frac{\vec{x}}{x_4^2} \right)^2 e^{-\vec{x}^2/2\gamma x_4} \vec{x}^2 \ \propto \ \int dx_4 \frac{1}{x_4}, \qquad (4.7)$$

which is logarithmically divergent in the ultraviolet. One can also readily check that this is the only term that has to be subtracted: The cubic Taylor term in the expansion of $\partial_s \tilde{G}^T$, Eq. (4.6), leads to a convergent contribution to the integral K.

In order to isolate the ultraviolet singularity in Eq. (4.7), we first cut out a sphere $\mathcal{S}$ of radius $|\mathcal{S}| \leqslant \beta/2$ around the origin and decompose the integral involving the contributions of class C as

$$
\int_{\mathcal{T}} d^{d_s+1}x \, \partial_r \Delta \partial_r \Delta \partial_s \tilde{G}^T \partial_s \tilde{G}^T
$$

$$
= \int_{\mathcal{S}} d^{d_s+1}x \, \partial_r \Delta \partial_r \Delta \partial_s \tilde{G}^T \partial_s \tilde{G}^T
$$

$$
+ \int_{\mathcal{T}\setminus\mathcal{S}} d^{d_s+1}x \, \partial_r \Delta \partial_r \Delta \partial_s \tilde{G}^T \partial_s \tilde{G}^T. \tag{4.8}
$$

In the limit $d_s \to 2$, the integral over the complement $\mathcal{T} \setminus \mathcal{S}$ of the sphere is not singular. The divergence is contained in the integral over the sphere. Here we subtract the singular term, (4.7), which leads us to

$$
\int_{\mathcal{S}} d^{d_s+1}x \, \partial_r \Delta(x) \partial_r \Delta(x) \partial_s G^T(-x) \partial_s G^T(-x)
$$

$$
= \int_{\mathcal{S}} d^{d_s+1}x \, \partial_r \Delta(x) \partial_r \Delta(x) Q_{ss}(x)
$$

$$
+ \int_{\mathcal{S}} d^{d_s+1}x \, \partial_r \Delta(x) \partial_r \Delta(x)
$$

$$
\times \partial_{\alpha s} G^T(-x)|_{x=0} \partial_{\beta s} G^T(-x)|_{x=0} x^\alpha x^\beta, \tag{4.9}
$$

where $Q_{ss}(x)$ is defined as

$$
Q_{ss}(x) = \partial_s G^T(-x) \partial_s G^T(-x)
$$

$$
- \partial_{\alpha s} G^T(-x)|_{x=0} \partial_{\beta s} G^T(-x)|_{x=0} x^\alpha x^\beta. \tag{4.10}
$$

The first integral on the right-hand side of Eq. (4.9) is now convergent. The second integral, however, is divergent in the ultraviolet. The last step in the isolation of this divergence consists in decomposing the singular integral as follows:

$$
\int_{\mathcal{S}} d^{d_s+1}x \, \partial_r \Delta(x) \partial_r \Delta(x) \partial_{\alpha s} G^T(-x)|_{x=0} \partial_{\beta s} G^T(-x)|_{x=0} x^\alpha x^\beta
$$

$$
= \int_{\mathcal{R}} d^{d_s+1}x \, \partial_r \Delta(x) \partial_r \Delta(x) \partial_{\alpha s} G^T(-x)|_{x=0}
$$

$$
\times \partial_{\beta s} G^T(-x)|_{x=0} x^\alpha x^\beta - \int_{\mathcal{R}\setminus\mathcal{S}} d^{d_s+1}x \, \partial_r \Delta(x) \partial_r \Delta(x)
$$

$$
\times \partial_{\alpha s} G^T(-x)|_{x=0} \partial_{\beta s} G^T(-x)|_{x=0} x^\alpha x^\beta. \tag{4.11}
$$

Now the ultraviolet singularity is contained in the integral over all Euclidean space, which can be written as

$$
\int_{\mathcal{R}} d^{d_s+1}x \, \partial_r \Delta(x) \partial_r \Delta(x) \partial_{\alpha s} G^T(-x)|_{x=0} \partial_{\beta s} G^T(-x)|_{x=0} x^\alpha x^\beta
$$

$$
= \frac{d_s(d_s+2)}{2^{3d_s+5} \pi^{\frac{3d_s}{2}} \gamma^{\frac{3d_s+4}{2}}} T^{d_s+2} (\mu H)^{\frac{d_s-2}{2}} \left\{ \sum_{n=1}^{\infty} \frac{e^{-\mu H n \beta}}{n^{\frac{d_s+2}{2}}} \right\}^2
$$

$$
\times \Gamma\left(1 - \frac{d_s}{2}\right). \tag{4.12}
$$

In the limit $d_s \to 2$, the above regularized expression is divergent because the Γ function develops a pole. Finally, we subtract this divergent expression from the integral K and define the renormalized integral $\bar{K}$ as

$$
\bar{K} = K - 2 \int_{\mathcal{R}} d^3x \, \partial_r \Delta(x) \partial_r \Delta(x) \partial_{\alpha s} G^T(-x)|_{x=0} \partial_{\beta s} G^T(-x)|_{x=0} x^\alpha x^\beta
$$

$$
= \int_{\mathcal{T}} d^3x \, (\partial_r G^T \partial_r G^T \partial_s \tilde{G}^T \partial_s \tilde{G}^T + 4 \partial_r \Delta \partial_r G^T \partial_s \tilde{G}^T \partial_s \tilde{G}^T) + 2 \int_{\mathcal{T}\setminus\mathcal{S}} d^3x \, \partial_r \Delta \partial_r \Delta \partial_s \tilde{G}^T \partial_s \tilde{G}^T + 2 \int_{\mathcal{S}} d^3x \, \partial_r \Delta \partial_r \Delta Q_{ss}
$$

$$
- 2 \int_{\mathcal{R}\setminus\mathcal{S}} d^3x \, \partial_r \Delta \partial_r \Delta \partial_{\alpha s} G^T(-x)|_{x=0} \partial_{\beta s} G^T(-x)|_{x=0} x^\alpha x^\beta. \tag{4.13}
$$

While the numerical evaluation of the finite expression $\bar{K}$ poses no problems and is considered in Appendix A, here we proceed with our discussion regarding the divergent piece in K. The point is that this divergence originating from the three-loop graph 8c can be canceled by an identical divergence in the two-loop graph 8d. More precisely, the divergence in the three-loop graph 8c can be absorbed into the next-to-leading-order effective constants l_1 and l_2 which come along with the two-loop graph 8d. This logarithmic renormalization of higher order effective constants is standard in a Lorentz-invariant framework. Indeed, the absorption of ultraviolet divergences occurring in loop graphs into next-to-leading-order effective constants was discussed a long time ago in the context of chiral perturbation theory, i.e., the low-energy effective theory of quantum chromodynamics.[47] Since the issue is rather technical, we do not present it in the main body of the paper; rather we relegate it to Appendix B.

Collecting all terms contributing to the free energy density up to order p^8, and writing the integral $\bar{K}$ as

$$
\bar{K}(\sigma) = T^4 \frac{k(\sigma)}{\gamma^5}, \quad \sigma = \mu H \beta = \frac{\mu H}{T}, \quad \gamma = \frac{F^2}{\Sigma}, \tag{4.14}
$$

the low-temperature expansion of the free energy density for the two-dimensional ideal ferromagnet finally takes the form

$$
z = -\Sigma \mu H - \frac{1}{4\pi\gamma} T^2 \sum_{n=1}^{\infty} \frac{e^{-\sigma n}}{n^2} - \frac{l_3}{\pi \Sigma \gamma^3} T^3 \sum_{n=1}^{\infty} \frac{e^{-\sigma n}}{n^3}
$$

$$
- \frac{3(4l_3^2 - c_1 \Sigma \gamma)}{\pi \Sigma^2 \gamma^5} T^4 \sum_{n=1}^{\infty} \frac{e^{-\sigma n}}{n^4} - \frac{8\bar{l}_1 + 6\bar{l}_2 + 5l_3}{24\pi^2 \Sigma^2 \gamma^4} T^4
$$

$$
\times \left\{ \sum_{n=1}^{\infty} \frac{e^{-\sigma n}}{n^2} \right\}^2 - \frac{k(\sigma)}{2\Sigma^2 \gamma^3} T^4 + \mathcal{O}(p^{10}). \tag{4.15}
$$

The quantities $\bar{l}_1$ and $\bar{l}_2$ are the renormalized next-to-leading-order effective constants (see Appendix B). Note that the next-to-leading-order effective constant l_3, much like the next-to-next-to-leading-order effective constant c_1, does not require renormalization; both quantities are finite as they stand.

While this series has been investigated before,[49–60] within both spin-wave theory and Schwinger-Boson mean field theory, we want to emphasize that all these references dealt with *free* magnons. The manifestation of the spin-wave interaction in the low-temperature expansion for the free energy density of the two-dimensional ideal ferromagnet is considered here. Furthermore, our rigorous approach is completely systematic and does not resort to any kind of approximations or *ad hoc* assumptions.

V. THERMODYNAMICS OF TWO-DIMENSIONAL IDEAL FERROMAGNETS

Using representation (4.15) for the free energy density we now discuss the thermodynamic properties of two-dimensional ideal ferromagnets. Let us first consider the low-temperature series for the pressure. Because the system is homogeneous, the pressure can be obtained from the temperature-dependent part of the free energy density:

$$P = z_0 - z. \tag{5.1}$$

Accordingly, up to order p^8, the low-temperature series for the pressure takes the form

$$P = \eta_0 T^2 + \eta_1 T^3 + \eta_2 T^4 + \mathcal{O}(p^{10}), \tag{5.2}$$

where the coefficients η_i are given by

$$\eta_0 = \frac{1}{4\pi\gamma} \sum_{n=1}^{\infty} \frac{e^{-\sigma n}}{n^2}, \quad \eta_1 = \frac{l_3}{\pi \Sigma \gamma^3} \sum_{n=1}^{\infty} \frac{e^{-\sigma n}}{n^3},$$

$$\eta_2 = \frac{3(4l_3^2 - c_1 \Sigma \gamma)}{\pi \Sigma^2 \gamma^5} \sum_{n=1}^{\infty} \frac{e^{-\sigma n}}{n^4} + \frac{8\bar{l}_1 + 6\bar{l}_2 + 5l_3}{24\pi^2 \Sigma^2 \gamma^4}$$

$$\times \left\{ \sum_{n=1}^{\infty} \frac{e^{-\sigma n}}{n^2} \right\}^2 + \frac{1}{2\Sigma^2 \gamma^3} k(\sigma). \tag{5.3}$$

Note that these coefficients depend on the dimensionless ratio $\sigma = \mu H/T$. Remarkably, the spin-wave interaction starts manifesting itself only at order $p^8 \propto T^4$ through the last two terms in the coefficient η_2. While the former contribution, which involves the renormalized effective constants $\bar{l}_1$ and $\bar{l}_2$, originates from a two-loop graph, the latter contribution, proportional to the dimensionless function $k(\sigma)$, comes from a three-loop graph. All other contributions in the pressure are related to one-loop graphs, i.e., to graphs that describe noninteracting magnons. In the above series for the pressure they contribute at order T^2, T^3, and T^4.

The ratio $\sigma = \mu H/T$ in the series for the pressure can take any value, provided that the temperature and the magnetic field are both small with respect to the intrinsic scale of the underlying theory. In the present case of the two-dimensional ideal ferromagnet, this scale may be identified with the exchange integral J of the Heisenberg model. In the following we are interested in the limit $T \gg \mu H$, which we implement by holding T fixed and sending the magnetic field to 0. By
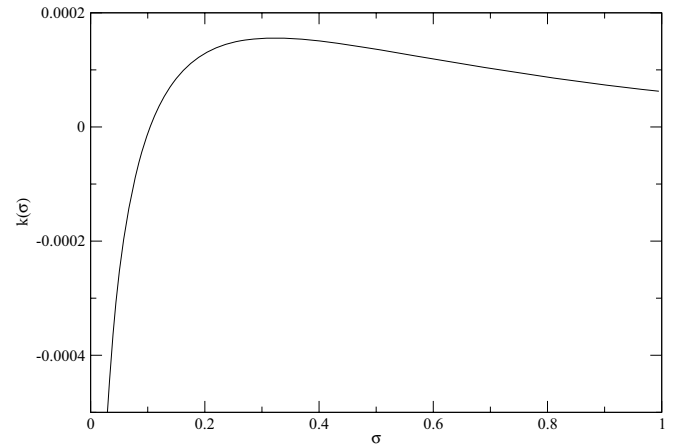

FIG. 2. The function $k(\sigma)$, where σ is the dimensionless parameter $\sigma = \mu H/T$.

keeping the fixed temperature low compared to the scale J, we thus never leave the domain of validity of the low-temperature effective expansion.

Formally, the limit $\sigma \to 0$ poses no problems for the one-loop contributions in the pressure. The corresponding coefficients in Eq. (5.3) become temperature independent and the sums reduce to Riemann ζ functions. However, one has to be very careful by taking this limit in the interaction part contained in the coefficient η_2. In order to address this issue, we first take a closer look at the dimensionless function $k(\sigma)$, which is depicted in Fig. 2.

In the limit $\sigma \to 0$, this function can be parametrized as

$$k(\sigma) = k_0 \ln \sigma + k_1 + k_2 \sigma \ln^2 \sigma + k_3 \sigma \ln \sigma + k_4 \sigma$$
$$+ \mathcal{O}(\sigma^2 \ln^3 \sigma), \tag{5.4}$$

where the coefficients k_i are pure numbers. Here we only need k_0 and k_1, which take the values

$$k_0 = \frac{\pi}{4608} = 6.818 \times 10^{-4}, \quad k_1 = 2.18 \times 10^{-3}. \tag{5.5}$$

The function $k(\sigma)$ thus diverges logarithmically, indicating that the limit $\sigma \to 0$ in the above representation for the pressure is rather subtle. In Appendix C it is shown that the sum of the two-loop and the three-loop contributions in the pressure,

$$\frac{8\bar{l}_1 + 6\bar{l}_2 + 5l_3}{24\pi^2 \Sigma^2 \gamma^4} \left\{ \sum_{n=1}^{\infty} \frac{e^{-\sigma n}}{n^2} \right\}^2 T^4 + \frac{1}{2\Sigma^2 \gamma^3} k(\sigma) T^4, \tag{5.6}$$

remains finite in the limit $\sigma \to 0$ and can be written as

$$\frac{k_0}{2\Sigma^2 \gamma^3} T^4 \ln \left(\frac{\Lambda_p}{T} \right) + \frac{5l_3}{24\pi^2 \Sigma^2 \gamma^4} \zeta(2)^2 T^4. \tag{5.7}$$

The quantity Λ_p is a scale which depends on the renormalized next-to-leading-order effective constants $\bar{l}_1$ and $\bar{l}_2$, as well as on the coefficients k_0 and k_1. In the absence of a magnetic field, the low-temperature expansion for the pressure of the

two-dimensional ideal ferromagnet hence takes the form

$$P = \frac{\zeta(2)}{4\pi\gamma}T^2 + \frac{l_3\zeta(3)}{\pi\Sigma\gamma^3}T^3 + \frac{3(4l_3^2 - c_1\Sigma\gamma)\zeta(4)}{\pi\Sigma^2\gamma^5}T^4$$
$$+ \frac{5l_3\zeta(2)^2}{24\pi^2\Sigma^2\gamma^4}T^4 + \frac{k_0}{2\Sigma^2\gamma^3}T^4\ln\left(\frac{\Lambda_p}{T}\right) + \mathcal{O}(p^{10}). \tag{5.8}$$

Interestingly, we are not dealing with a simple power series. At order p^8, where the spin-wave interaction sets in, a logarithmic contribution $T^4\ln T$ emerges. Although this term contains a scale related to next-to-leading-order effective constants of $\mathcal{L}_{\text{eff}}^4$, the coefficient of this term is fixed by the effective constants Σ and F of the leading-order Lagrangian $\mathcal{L}_{\text{eff}}^2$ and by the quantity k_0, which is a pure number.

In a Lorentz-invariant setting, the occurrence of such logarithmic terms is well known. The low-temperature expansion of the pressure in quantum chromodynamics involves the term $T^8\ln T$ in the chiral limit[6]. In fact, the term $T^8\ln T$ also occurs in the low-temperature expansion of the pressure of the three-dimensional antiferromagnet in the absence of a staggered field.[7] Note that antiferromagnetic magnons, much like pions in quantum chromodynamics, display a linear, i.e., relativistic dispersion law.

While the limit $H \to 0$ in the interaction contribution turned out to be rather subtle, one may have doubts in general about switching off the magnetic field. After all, we are dealing with a planar system, where we are facing the Mermin-Wagner theorem. However, as shown in Ref. 1, switching off the magnetic field in the low-temperature series for the pressure does not really numerically affect the series. We discuss the issue in more detail in the next section, where we consider the magnetization.

For the reader's convenience, in Appendix D we provide the low-temperature series for the energy density u, the entropy density s, and the heat capacity c_V of the two-dimensional ideal ferromagnet. We want to stress that the structure of the various low-temperature series derived in this section and in Appendix D is an immediate consequence of the symmetries of the two-dimensional ideal ferromagnet. Unlike spin-wave theory or Schwinger-Boson mean field theory, the effective Lagrangian technique does not resort to any *ad hoc* assumptions or approximations but is completely systematic. Moreover, the manifestation of the spin-wave interaction in the low-temperature series of the partition function of the two-dimensional ideal ferromagnet is studied here. In particular, addressing this problem with spin-wave theory or Schwinger-Boson mean field theory up to the order considered in the present analysis appears to be beyond reach.

At the end of this section, we compare the low-temperature expansions for the free energy density of the ideal ferromagnet in two and three spatial dimensions. In the absence of an external magnetic field they exhibit the general structure

$$z_{d_s=2} = -\tilde{\eta}_0 T^2 - \tilde{\eta}_1 T^3 - \tilde{\eta}_2^{\mathbf{A}}\mathbf{T^4} + \tilde{\eta}_2^{\mathbf{B}}\mathbf{T^4 \ln T} + \mathcal{O}(\mathbf{p^{10}}),$$
$$z_{d_s=3} = -\tilde{h}_0 T^{\frac{5}{2}} - \tilde{h}_1 T^{\frac{7}{2}} - \tilde{h}_2 T^{\frac{9}{2}} - \tilde{\mathbf{h}}_3\mathbf{T^5} - \tilde{\mathbf{h}}_4\mathbf{T^{11/2}} + \mathcal{O}(\mathbf{p^{12}}),$$
$$\tag{5.9}$$

where we have boldfaced all contributions which are related to the spin-wave interaction. Note that in the case of the

two-dimensional ideal ferromagnet, the coefficient $\tilde{\eta}_2$ has two parts. The former one, $\tilde{\eta}_2^A$, contains the free magnon part as well as the interaction contribution proportional to l_3. The latter one, $\tilde{\eta}_2^B$, is exclusively due to the spin-wave interaction, which involves the renormalized next-to-leading-order effective constants $\bar{l}_1$ and $\bar{l}_2$.

In three dimensions, the term of order $T^5 \propto p^{10}$ in the free energy density is the famous Dyson interaction term; in the effective framework this is a two-loop effect (see Ref. 4). Corrections to the Dyson term were considered in Ref. 5, pointing out that the leading correction is of order $T^{11/2} \propto p^{11}$ and originates from a three-loop graph. Interestingly, in the case of the three-dimensional ideal ferromagnet, the two-loop and the three-loop contributions occur at different orders in the low-temperature expansion. As we have outlined in the present article, the same two-loop and three-loop graphs, in the case of the two-dimensional ideal ferromagnet, all contribute at the same order p^8 and lead to a logarithmic term $T^4\ln T$ in the free energy density. As argued in Ref. 1, the different organization of Feynman diagrams in three and two spatial dimensions is a consequence of the suppression of ferromagnetic loops in Feynman graphs: In three spatial dimensions, each loop in a Feynman diagram is suppressed by three powers of momentum. In two dimensions, on the other hand, ferromagnetic loops are only suppressed by two powers of momentum.

VI. MAGNETIZATION AND MERMIN-WAGNER THEOREM

Let us now consider the magnetization. With the expression for the free energy density, (4.15), the low-temperature expansion for the magnetization,

$$\Sigma(T,H) = -\frac{\partial z}{\partial(\mu H)}, \tag{6.1}$$

of the two-dimensional ideal ferromagnet takes the form

$$\frac{\Sigma(T,H)}{\Sigma} = 1 - \hat{\alpha}_0 T - \hat{\alpha}_1 T^2 - \hat{\alpha}_2 T^3 + \mathcal{O}(p^8). \tag{6.2}$$

The coefficients $\hat{\alpha}_i$ depend on the dimensionless ratio $\sigma = \mu H/T$ and are given by

$$\hat{\alpha}_0 = \frac{1}{4\pi\gamma\Sigma}\sum_{n=1}^{\infty}\frac{e^{-\sigma n}}{n}, \quad \hat{\alpha}_1 = \frac{l_3}{\pi\Sigma^2\gamma^3}\sum_{n=1}^{\infty}\frac{e^{-\sigma n}}{n^2},$$

$$\hat{\alpha}_2 = \frac{3(4l_3^2 - c_1\Sigma\gamma)}{\pi\Sigma^3\gamma^5}\sum_{n=1}^{\infty}\frac{e^{-\sigma n}}{n^3} + \frac{8\bar{l}_1 + 6\bar{l}_2 + 5l_3}{12\pi^2\Sigma^3\gamma^4}$$

$$\times \sum_{m=1}^{\infty}\frac{e^{-\sigma m}}{m}\sum_{n=1}^{\infty}\frac{e^{-\sigma n}}{n^2} - \frac{1}{2\Sigma^3\gamma^3}\frac{dk(\sigma)}{d\sigma}. \tag{6.3}$$

Obviously this series has a problem if we want to switch off the magnetic field, as the leading coefficient $\hat{\alpha}_0$ then diverges. The point is that it is completely inconsistent to take the limit $\sigma \to 0$ in the low-temperature expansion of the magnetization, as we now discuss.

We should keep in mind that the present effective calculation is based on the assumption that the internal spin symmetry O(3) is spontaneously broken. While this assumption is fulfilled at zero temperature, at finite tempera-

ture spontaneous symmetry breaking in the two-dimensional Heisenberg ferromagnet cannot occur according to the Mermin-Wagner theorem.[61] Rather, at finite temperature, the low-energy spectrum of the two-dimensional ideal ferromagnet exhibits a nonperturbatively generated energy gap and the correlation length of the magnons, although still exponentially large,[63]

$$\xi_{np} = C_\xi a S^{-\frac{1}{2}} \sqrt{\frac{T}{JS^2}} \exp\left[\frac{2\pi JS^2}{T}\right], \qquad (6.4)$$

is no longer infinite.

We have mentioned before that these nonperturbative effects are so tiny that they cannot manifest themselves in the low-temperature series for the free energy density. Likewise, the series for the pressure, the energy density, the entropy density, and the heat capacity derived in the previous section are also valid as they stand; the subtleties raised by the Mermin-Wagner theorem are not relevant for these thermodynamic quantities.

However, for the magnetization, matters are quite different. There, the nonperturbatively generated energy gap does not lead to tiny corrections in the low-temperature expansion; rather these effects become the dominant ones. We can easily see this by expanding the series in the small parameter $\sigma = \mu H/T$. While the free energy density amounts to

$$z = -\Sigma\mu H - \frac{T^2}{4\pi\gamma}\left\{\zeta(2) + \sigma\ln\sigma - \sigma - \frac{\sigma^2}{4} + \mathcal{O}(\sigma^3)\right\} + \mathcal{O}(T^3), \qquad (6.5)$$

the magnetization takes the form

$$\Sigma(T,H) = \Sigma + \frac{T}{4\pi\gamma}\left\{\ln\sigma - \frac{\sigma}{2} + \frac{\sigma^2}{24} + \mathcal{O}(\sigma^4)\right\} + \mathcal{O}(T^2). \qquad (6.6)$$

In the effective theory perspective, the quantity ΔE_H,

$$\Delta E_H = \mu H, \qquad (6.7)$$

is the energy gap induced by the weak external magnetic field; this is the quantity that appears in the parameter σ. However, there is a further mechanism contributing to the energy gap, the one that generates a gap nonperturbatively. In analogy to the definition of the correlation length, related to the energy gap ΔE_H,[1]

$$\xi = \sqrt{\frac{\gamma}{\mu H}} = \sqrt{\frac{\gamma}{\Delta E_H}}, \qquad (6.8)$$

the nonperturbatively generated energy gap ΔE_{np} is connected to the correlation length ξ_{np} by

$$\Delta E_{np} = \frac{\gamma}{\xi_{np}^2}. \qquad (6.9)$$

In our low-temperature series, so far only the energy gap ΔE_H is accounted for in the parameter σ.

We have to remember that we implement the limit $T \gg \mu H$ by holding T fixed and sending the magnetic field to 0. Keeping the fixed temperature low compared to the underlying scale given by the exchange integral J, we never leave the domain of validity of the effective low-temperature expansion. Now for a

fixed value of the temperature, the nonperturbatively generated energy gap ΔE_{np} is just a constant. However, unlike the energy gap induced by the external magnetic field, the generation of ΔE_{np} is a dynamical effect that we cannot control. In particular, while we can switch off the magnetic field and thus ΔE_H, we cannot switch off ΔE_{np}; it would be inconsistent to consider values for σ smaller than $\sigma_{np} = \Delta E_{np}/T$ in the effective low-temperature series.

At very low temperatures—let us say $T/J = 1/100$—relations (6.4) and (6.8) imply that the condition

$$\Delta E_{np} = \Delta E_H \qquad (6.10)$$

is satisfied if the ratio $\mu H/T$ takes the value

$$\frac{\mu H}{T} = \frac{10^4}{16C_\xi^2} e^{-100\pi} \approx 10^{-131} \quad \left(S = \frac{1}{2}\right). \qquad (6.11)$$

This tiny ratio thus leads to a negligible contribution to the free energy density, (6.5); here, although conceptually inconsistent, taking the limit $\sigma \to 0$ does not numerically affect the series. However, in the magnetization, (6.6), the effect of the nonperturbatively generated energy gap is rather large because of the logarithm $\ln\sigma$; taking the limit $\sigma \to 0$ in the magnetization would be completely inconsistent.

In conclusion, at nonzero temperature the nonperturbatively generated correlation length is finite and there is always an energy gap ΔE_{np} in the spectrum of the two-dimensional ideal ferromagnet. The question is whether or not this gap is numerically relevant in the low-temperature series: For the thermodynamic quantities it is irrelevant; for the magnetization, however, it is indeed relevant.

The low-temperature expansion of the magnetization of two-dimensional ideal ferromagnets has been considered before within the formalism of double-time-temperature Green's functions and spin-wave theory. The explicit expressions given in Refs. [59] and [60], respectively, are consistent with our effective analysis provided that we express the effective constants γ and l_3 in terms of microscopic constants as[1]

$$\gamma = JSa^2, \quad l_3 = \frac{JS^2a^2}{32}. \qquad (6.12)$$

Here J is the exchange integral of the Heisenberg model and a is the distance between the sites on the square lattice.

We have to emphasize, however, that Refs. [59] and [60] were restricted to *free* magnons. The effect of the spin-wave interaction on the low-temperature expansion of the magnetization of two-dimensional ideal ferromagnets has been considered for the first time in the present work.

VII. CONCLUSIONS

Using the method of effective Lagrangians, we have evaluated the partition function of the two-dimensional ideal ferromagnet up to three loops and have derived the low-temperature series for various thermodynamic quantities including the magnetization. In particular, we have shown that in the absence of an external magnetic field, the spin-wave interaction starts manifesting itself in the form of a logarithmic term $T^4 \ln T$ in the free energy density. To obtain this result,

we had to renormalize and numerically evaluate a specific three-loop graph which turned out to be the piece of resistance. Much like in the case of three-dimensional ideal ferromagnets, the spin-wave interaction is also very weak in two-dimensional ideal ferromagnets.

We have discussed in detail the implications of the Mermin-Wagner theorem for the low-temperature series derived in the present work. While the series for the free energy density, pressure, internal energy density, entropy density, and heat capacity are also valid if the magnetic field is switched off, one has to be careful in the case of the magnetization, where the effect of the nonperturbatively generated energy gap cannot be neglected.

Although various authors have considered the low-temperature properties of two-dimensional ideal ferromagnets before within spin-wave theory, Schwinger-Boson mean field theory, and double-time-temperature Green's functions, to the best of our knowledge, they all restricted themselves to free magnons. In particular, none of those authors identified logarithmic terms in the low-temperature expansion of the partition function. The systematic effective field theory method thus proves to be more powerful than conventional condensed matter methods, where a three-loop analysis appears to be beyond reach.

Such logarithmic terms are well known in particle physics, i.e., in chiral perturbation theory which is the effective field theory of the strong interaction described by quantum chromodynamics. They also occur in the context of the three-dimensional antiferromagnet, whose spin waves obey a linear (relativistic) dispersion law. These logarithmic terms are a consequence of the structure of the ultraviolet divergences in the Goldstone boson propagator. In quantum chromodynamics, in the case of three-dimensional antiferromagnets as well as two-dimensional ideal ferromagnets, these divergences can be absorbed into next-to-leading-order effective constants by logarithmic renormalization. Interestingly, in the case of the three-dimensional ideal ferromagnet, the ultraviolet divergences of the propagator do not require logarithmic renormalization:[5] The low-temperature series for the thermodynamic quantities and the magnetization simply involve integer and half-integer powers of the temperature.

The present study regarding the low-temperature properties of two-dimensional ideal ferromagnets is on the same footing as the analysis performed in Ref. 5, which dealt with three-dimensional ideal ferromagnets. In both cases a complete and systematic analysis of the partition functions was given up to three-loop order. In the three-dimensional case, the effect of the spin-wave interaction on the partition function has been considered by numerous authors before, in particular, by Dyson, in his monumental work.[2] The effective three-loop analysis presented in Ref. 5 went one step beyond Dyson. And the present article has discussed the effect of the spin-wave interaction on the partition function in the case of the two-dimensional ideal ferromagnet.

APPENDIX A: NUMERICAL EVALUATION OF THE CATEYE GRAPH

In this Appendix, we consider the numerical evaluation of the three-loop graph 8c. The various terms in the relevant expression $\bar{K}$, defined in Eq. (4.13), only involve the variables $r = |\vec{x}|$ and $t = x_4$, such that the integrals in fact become two-dimensional:

$$d^3x = 2\pi r\, dr\, dt. \tag{A1}$$

A very welcome consistency check on the numerics is provided by the fact that the result has to be independent of the radius of the sphere $\mathcal{S}$.

It is convenient to introduce the dimensionless integration variables η and ξ,

$$\eta = T x_4, \quad \xi = \frac{1}{2}\sqrt{\frac{T}{\gamma}}|\vec{x}|. \tag{A2}$$

In the integrals over the torus which involve quartic and triple sums—the first two terms in Eq. (4.13)—we first integrate over all two-dimensional space, ending up with one-dimensional integrals in the variable η. For the quartic sum we obtain

$$\int_{\mathcal{T}} d^3x\, \partial_r G^T(x)\partial_r G^T(x)\partial_s G^T(-x)\partial_s G^T(-x)$$

$$= \frac{1}{32\pi^3\gamma^5} T^4 \int_{-1/2}^{1/2} d\eta \sum_{n_1\ldots n_4=1}^{\infty} e^{-\sigma(n_1+n_2+n_3+n_4)}$$

$$\times \hat{Q}(\eta,n_1,n_2,n_3,n_4),$$

$$\hat{Q}(\eta,n_1,n_2,n_3,n_4)$$

$$= \frac{\left(\frac{1}{\eta+n_1} + \frac{1}{\eta+n_2} + \frac{1}{-\eta+n_3} + \frac{1}{-\eta+n_4}\right)^{-3}}{((\eta+n_1)(\eta+n_2)(-\eta+n_3)(-\eta+n_4))^2}, \tag{A3}$$

while for the triple sum we get

$$\int_{\mathcal{T}} d^3x\, \partial_r \Delta(x)\partial_r G^T(x)\partial_s G^T(-x)\partial_s G^T(-x)$$

$$= \frac{1}{32\pi^3\gamma^5} T^4 \int_0^{1/2} d\eta \sum_{n_2\ldots n_4=1}^{\infty} e^{-\sigma(n_2+n_3+n_4)}$$

$$\times \hat{Q}(\eta,0,n_2,n_3,n_4),$$

$$\hat{Q}(\eta,0,n_2,n_3,n_4)$$

$$= \frac{\left(\frac{1}{\eta} + \frac{1}{\eta+n_2} + \frac{1}{-\eta+n_3} + \frac{1}{-\eta+n_4}\right)^{-3}}{(\eta(\eta+n_2)(-\eta+n_3)(-\eta+n_4))^2}, \tag{A4}$$

where

$$\sigma = \frac{\mu H}{T}, \quad \gamma = \frac{F^2}{\Sigma}. \tag{A5}$$

In the case of the triple sums the integration over η only extends over the interval $[0,\frac{1}{2}]$, due to the Θ function contained in the zero-temperature propagator $\Delta(x)$.

Note that the quantities $\hat{Q}(\eta,n_1,n_2,n_3,n_4)$ and $\hat{Q}(\eta,0,n_2,n_3,n_4)$ depend in a rather nontrivial manner on the summation variables. The slowest convergence for expressions (A3) and (A4) is observed for $\sigma = 0$, because no exponential damping occurs. The numerical summation has been performed in a "Cartesian" way as follows. We first define the vector $\vec{N}_i = (n_1,n_2,n_2,n_4)$. The first partial sum S_1

in the quartic series simply corresponds to the combination $\vec{N}_1 = (1,1,1,1)$ of indices. The second partial sum S_2 then contains all combinations of indices in the vector $\vec{N}_2$ with at least one index equal to 2: $(2,1,1,1), \ldots, (2,2,2,2)$, etc. For large values of i and for $\sigma = 0$, the partial sums S_i converge according to $1/S_i^2$. Proceeding in an analogous manner for the triple sums, the asymptotic behavior turns out to be the same.

Expressions suitable for the numerical evaluation of the remaining three integrals in Eq. (4.13) involving double sums are

$$
\int_{\mathcal{T}\backslash\mathcal{S}} d^3x\, \partial_r \Delta(x) \partial_r \Delta(x) \partial_s G^T(-x) \partial_s G^T(-x)
$$
$$
= \frac{1}{32\pi^3\gamma^5} T^4 \int_0^S d\eta \int_{\sqrt{S^2-\eta^2}}^\infty d\xi\, \xi^5
$$
$$
\times \sum_{n_1,n_2=1}^\infty e^{-\sigma(n_1+n_2)}\, \hat{P}(\xi,\eta,n_1,n_2),
$$
$$
\hat{P}(\xi,\eta,n_1,n_2) = \frac{e^{-\xi^2\left(\frac{2}{\eta}+\frac{1}{-\eta+n_1}+\frac{1}{-\eta+n_2}\right)}}{\{\eta^2(-\eta+n_1)(-\eta+n_2)\}^2}, \tag{A6}
$$

$$
\int_{\mathcal{S}} d^3x\, \partial_r \Delta(x) \partial_r \Delta(x) Q_{ss}(x)
$$
$$
= \frac{1}{32\pi^3\gamma^5} T^4 \int_0^S d\eta \int_0^{\sqrt{S^2-\eta^2}} d\xi\, \xi^5
$$
$$
\times \sum_{n_1,n_2=1}^\infty e^{-\sigma(n_1+n_2+2\eta)}\, \hat{Q}(\xi,\eta,n_1,n_2,\sigma), \tag{A7}
$$

with

$$
\hat{Q}(\xi,\eta,n_1,n_2,\sigma) = e^{-\xi^2\left(\frac{2}{\eta}+\frac{1}{-\eta+n_1}+\frac{1}{-\eta+n_2}\right)}
$$
$$
\times \frac{\frac{e^{2\eta\sigma}}{\{(-\eta+n_1)(-\eta+n_2)\}^2} - \frac{e^{\xi^2\left(\frac{-1}{-\eta+n_1}+\frac{-1}{-\eta+n_2}\right)}}{n_1^2 n_2^2}}{\eta^4},
$$
$$
\tag{A8}
$$

and, finally,

$$
\int_{\mathcal{R}\backslash\mathcal{S}} d^3x\, \partial_r \Delta(x) \partial_r \Delta(x) \partial_{s\alpha} G^T(-x)|_{x=0} x^\alpha \partial_{s\beta} G^T(-x)|_{x=0} x^\beta
$$
$$
= \frac{1}{32\pi^3\gamma^5} T^4 \int_S^\infty d\eta \int_0^\infty d\xi\, \xi^5
$$
$$
\times \sum_{n_1,n_2=1}^\infty e^{-\sigma(n_1+n_2+2\eta)}\, \hat{R}(\xi,\eta,n_1,n_2)
$$
$$
+ \frac{1}{32\pi^3\gamma^5} T^4 \int_0^S d\eta \int_{\sqrt{S^2-\eta^2}}^\infty d\xi\, \xi^5
$$
$$
\times \sum_{n_1,n_2=1}^\infty e^{-\sigma(n_1+n_2+2\eta)}\, \hat{R}(\xi,\eta,n_1,n_2),
$$
$$
\hat{R}(\xi,\eta,n_1,n_2) = \frac{e^{-2\xi^2/\eta}}{\{\eta^2 n_1 n_2\}^2}. \tag{A9}
$$

In the above integrals the radius of the sphere has been chosen as $S = \frac{1}{2}$. For large values of i and for $\sigma = 0$, the partial sums S_i related to the above three expressions involving double sums converge according to $1/S_i^2$, i.e., the asymptotic behavior is the same as for the triple and quartic sums.

APPENDIX B: LOGARITHMIC RENORMALIZATION OF THE EFFECTIVE CONSTANTS l_1 AND l_2

In this Appendix we discuss how the ultraviolet divergence in

$$
\int_{\mathcal{R}} d^{d_s+1}x\, \partial_r \Delta(x) \partial_r \Delta(x) \partial_{\alpha s} G^T(-x)|_{x=0} \partial_{\beta s} G^T(-x)|_{x=0}
$$
$$
\times x^\alpha x^\beta = \frac{d_s(d_s+2)}{2^{3d_s+5}\pi^{\frac{3d_s}{2}}\gamma^{\frac{3d_s+4}{2}}} T^{d_s+2}(\mu H)^{\frac{d_s-2}{2}}
$$
$$
\times \left\{ \sum_{n=1}^\infty \frac{e^{-\mu H n\beta}}{n^{\frac{d_s+2}{2}}} \right\}^2 \Gamma\left(1-\frac{d_s}{2}\right), \tag{B1}
$$

originating from the three-loop graph 8c (Fig. 1), can be absorbed into the next-to-leading effective constants l_1 and l_2 which show up in the two-loop contribution $z_{8[de]}^T$:

$$
z_{8[de]}^T = -\frac{8l_1 + 6l_2 + 5l_3}{24\pi^2\Sigma^2\gamma^4} T^4 \left(\sum_{n=1}^\infty \frac{e^{-\mu H n\beta}}{n^2} \right)^2. \tag{B2}
$$

The singularity in Eq. (B1) is due to the Γ function, which contains a pole at $d_s = 2$,

$$
\Gamma\left(1-\frac{d_s}{2}\right) = -\frac{2}{d_s-2} - \gamma_E + \mathcal{O}(d_s-2), \tag{B3}
$$

where γ_E is Euler's constant.

Now the two expressions (B1) and (B2) have the same structure. They both involve the same infinite series and are both proportional to four powers of the temperature. Taking into account the prefactor of the integral $\bar{K}$ from Eq. (3.25), they add up to

$$
-\frac{1}{24\pi^2\Sigma^2\gamma^3} \left\{ \frac{8l_1 + 6l_2 + 5l_3}{\gamma} \right.
$$
$$
\left. + \frac{3}{32\pi} \Gamma\left(1-\frac{d_s}{2}\right)(\mu H)^{\frac{d_s-2}{2}} \right\} T^4 \left(\sum_{n=1}^\infty \frac{e^{-\mu H n\beta}}{n^2} \right)^2. \tag{B4}
$$

The pole in the Γ function can thus be absorbed into the combination $8l_1 + 6l_2 + 5l_3$ of next-to-leading-order effective constants. Note, however, that l_3 does not require renormalization. This effective constant already occurred in the one-loop result for the free energy density, (3.1), and is perfectly finite. The combination $8l_1 + 6l_2$, on the other hand, is divergent and absorbs the pole in the Γ function as we now show explicitly.

Introducing an arbitrary renormalization scale $\tilde{\mu}$, which should not be confused with the symbol μ denoting the magnetic moment, the divergent quantity λ,

$$
\lambda = \Gamma\left(1-\frac{d_s}{2}\right)(\mu H)^{\frac{d_s-2}{2}}, \tag{B5}
$$

can be decomposed into

$$
\lambda = \Gamma\left(1-\frac{d_s}{2}\right)\tilde{\mu}^{\frac{d_s-2}{2}} + \Gamma\left(1-\frac{d_s}{2}\right)\left[(\mu H)^{\frac{d_s-2}{2}} - \tilde{\mu}^{\frac{d_s-2}{2}}\right].
$$
$$
\tag{B6}
$$

The first term contains the singularity. Note that it does not involve the magnetic field but depends on the arbitrary renormalization scale $\tilde{\mu}$. The second term is not singular in the

limit $d_s \to 2$ but approaches the finite value

$$-\ln\left(\frac{\mu H}{\tilde{\mu}}\right), \tag{B7}$$

such that the sum, (B4), takes the form

$$-\frac{1}{24\pi^2\Sigma^2\gamma^3}\left\{\frac{8\bar{l}_1(\tilde{\mu})+6\bar{l}_2(\tilde{\mu})+5l_3}{\gamma}-\frac{3}{32\pi}\ln\left(\frac{\mu H}{\tilde{\mu}}\right)\right\}$$

$$\times T^4\left(\sum_{n=1}^{\infty}\frac{e^{-\mu H n\beta}}{n^2}\right)^2. \tag{B8}$$

The quantities $\bar{l}_1(\tilde{\mu})$ and $\bar{l}_2(\tilde{\mu})$ are the renormalized, i.e., finite, effective constants which depend on the renormalization scale $\tilde{\mu}$. It is important to note, however, that the curly brace is independent of this scale. Moreover, if we choose the renormalization scale as

$$\tilde{\mu} = \mu H \equiv \frac{J}{10}, \tag{B9}$$

then the logarithm drops out and it is understood that $\bar{l}_1(\tilde{\mu})$ and $\bar{l}_2(\tilde{\mu})$ are the renormalized effective constants evaluated at this specific choice of the scale. The choice that $\tilde{\mu}$ be one-tenth of the underlying scale given by the exchange integral J is motivated by comparison with chiral perturbation theory. There, in order for the logarithm to drop out, the scale is to be identified with the pion mass M, which is about one order of magnitude smaller than the underlying scale Λ_{QCD}.

From a more practical point of view we can say that the net effect of this whole renormalization procedure is simply this: The divergence in Eq. (B1) can be taken care of by rewriting the expression $z_{8[de]}^T$ in terms of the two renormalized effective constants $\bar{l}_1$ and $\bar{l}_2$ evaluated at the renormalization scale $\tilde{\mu} = \mu H$ as

$$z_{8[de]}^T = -\frac{8\bar{l}_1+6\bar{l}_2+5l_3}{24\pi^2\Sigma^2\gamma^4}T^4\left(\sum_{n=1}^{\infty}\frac{e^{-\mu H n\beta}}{n^2}\right)^2. \tag{B10}$$

APPENDIX C: PRESSURE AT ZERO MAGNETIC FIELD

In this Appendix, we discuss the low-temperature expansion for the pressure at zero magnetic field. While this limit in the one-loop contributions formally poses no problems, switching off the magnetic field in the interaction contribution

of order p^8,

$$\frac{8\bar{l}_1+6\bar{l}_2+5l_3}{24\pi^2\Sigma^2\gamma^4}\left\{\sum_{n=1}^{\infty}\frac{e^{-\sigma n}}{n^2}\right\}^2 T^4 + \frac{1}{2\Sigma^2\gamma^3}k(\sigma)T^4, \tag{C1}$$

is rather subtle. Using representation (5.4) for the dimensionless function $k(\sigma)$, the interaction contribution, in the limit $H \to 0$, amounts to

$$\frac{k_0}{2\Sigma^2\gamma^3}\left\{\frac{\pi^2(8\bar{l}_1+6\bar{l}_2+5l_3)}{432\gamma k_0}+\ln\left(\frac{\mu H}{T}\right)+\frac{k_1}{k_0}\right\}T^4. \tag{C2}$$

The effective constants $\bar{l}_1, \bar{l}_2,$ and l_3 have the same dimension as $\gamma = F^2/\Sigma$. For reasons which become obvious in a moment, we write the renormalized effective constants as

$$\bar{l}_1 \equiv \gamma c \ln\left(\frac{\Lambda_1}{\mu H}\right)^{\frac{1}{16}}, \quad \bar{l}_2 \equiv \gamma c \ln\left(\frac{\Lambda_2}{\mu H}\right)^{\frac{1}{12}}, \quad c \equiv \frac{432k_0}{\pi^2}, \tag{C3}$$

where we have introduced the two scales Λ_1 and Λ_2, which are independent of the magnetic field. Inserting this representation for $\bar{l}_1$ and $\bar{l}_2$ into the first term in the curly brace in expression (C2), one obtains

$$\frac{k_0}{2\Sigma^2\gamma^3}\left\{\ln\left(\frac{\Lambda_p}{\mu H}\right)+\ln\left(\frac{\mu H}{T}\right)+\frac{5\pi^2l_3}{432\gamma k_0}\right\}T^4, \tag{C4}$$

where the scale Λ_p is given by

$$\Lambda_p = \sqrt{\Lambda_1\Lambda_2}\, e^{k_1/k_0} \approx 24.5\sqrt{\Lambda_1\Lambda_2}. \tag{C5}$$

The essential point is that in the sum, (C4), the magnetic field drops out. We conclude that, if one switches off the magnetic field in the low-temperature expansion for the pressure, the interaction contribution does not just manifest itself in the form of a simple power of the temperature; rather, it also involves a logarithmic contribution, which reads

$$\frac{k_0}{2\Sigma^2\gamma^3}T^4\ln\left(\frac{\Lambda_p}{T}\right). \tag{C6}$$

APPENDIX D: LOW-TEMPERATURE SERIES FOR ENERGY DENSITY, ENTROPY DENSITY, AND HEAT CAPACITY

In this final Appendix, let us derive the low-temperature series for the energy density u, the entropy density s, and the heat capacity c_V of the two-dimensional ideal ferromagnet. They are readily worked out from the thermodynamic relations

$$s = \frac{\partial P}{\partial T}, \quad u = Ts - P, \quad c_V = \frac{\partial u}{\partial T} = T\frac{\partial s}{\partial T} \tag{D1}$$

and amount to

$$u = \frac{1}{4\pi\gamma}T^2\left\{\sum_{n=1}^{\infty}\frac{e^{-\sigma n}}{n^2}+\sigma\sum_{n=1}^{\infty}\frac{e^{-\sigma n}}{n}\right\}+\frac{l_3}{\pi\Sigma\gamma^3}T^3\left\{2\sum_{n=1}^{\infty}\frac{e^{-\sigma n}}{n^3}+\sigma\sum_{n=1}^{\infty}\frac{e^{-\sigma n}}{n^2}\right\}+\frac{3(4l_3^2-c_1\Sigma\gamma)}{\pi\Sigma^2\gamma^5}T^4$$

$$\times\left\{3\sum_{n=1}^{\infty}\frac{e^{-\sigma n}}{n^4}+\sigma\sum_{n=1}^{\infty}\frac{e^{-\sigma n}}{n^3}\right\}+\frac{8\bar{l}_1+6\bar{l}_2+5l_3}{24\pi^2\Sigma^2\gamma^4}T^4\left\{3\sum_{m=1}^{\infty}\frac{e^{-\sigma m}}{m^2}\sum_{n=1}^{\infty}\frac{e^{-\sigma n}}{n^2}+2\sigma\sum_{m=1}^{\infty}\frac{e^{-\sigma m}}{m}\sum_{n=1}^{\infty}\frac{e^{-\sigma n}}{n^2}\right\}$$

$$+\frac{1}{2\Sigma^2\gamma^3}T^4\left\{3k(\sigma)-\sigma\frac{dk(\sigma)}{d\sigma}\right\}+\mathcal{O}(p^{10}),$$

$$s = \frac{1}{4\pi\gamma}T\left\{2\sum_{n=1}^{\infty}\frac{e^{-\sigma n}}{n^2} + \sigma\sum_{n=1}^{\infty}\frac{e^{-\sigma n}}{n}\right\} + \frac{l_3}{\pi\Sigma\gamma^3}T^2\left\{3\sum_{n=1}^{\infty}\frac{e^{-\sigma n}}{n^3} + \sigma\sum_{n=1}^{\infty}\frac{e^{-\sigma n}}{n^2}\right\} + \frac{3\left(4l_3^2 - c_1\Sigma\gamma\right)}{\pi\Sigma^2\gamma^5}T^3$$

$$\times\left\{4\sum_{n=1}^{\infty}\frac{e^{-\sigma n}}{n^4} + \sigma\sum_{n=1}^{\infty}\frac{e^{-\sigma n}}{n^3}\right\} + \frac{8\bar{l}_1 + 6\bar{l}_2 + 5l_3}{12\pi^2\Sigma^2\gamma^4}T^3\left\{2\sum_{m=1}^{\infty}\frac{e^{-\sigma m}}{m^2}\sum_{n=1}^{\infty}\frac{e^{-\sigma n}}{n^2} + \sigma\sum_{m=1}^{\infty}\frac{e^{-\sigma m}}{m}\sum_{n=1}^{\infty}\frac{e^{-\sigma n}}{n^2}\right\}$$

$$+ \frac{1}{2\Sigma^2\gamma^3}T^3\left\{4k(\sigma) - \sigma\frac{dk(\sigma)}{d\sigma}\right\} + \mathcal{O}(p^8),$$

$$c_V = \frac{1}{4\pi\gamma}T\left\{2\sum_{n=1}^{\infty}\frac{e^{-\sigma n}}{n^2} + 2\sigma\sum_{n=1}^{\infty}\frac{e^{-\sigma n}}{n} + \sigma^2\sum_{n=1}^{\infty}e^{-\sigma n}\right\} + \frac{l_3}{\pi\Sigma\gamma^3}T^2\left\{6\sum_{n=1}^{\infty}\frac{e^{-\sigma n}}{n^3} + 4\sigma\sum_{n=1}^{\infty}\frac{e^{-\sigma n}}{n^2} + \sigma^2\sum_{n=1}^{\infty}\frac{e^{-\sigma n}}{n}\right\}$$

$$+ \frac{3(4l_3^2 - c_1\Sigma\gamma)}{\pi\Sigma^2\gamma^5}T^3\left\{12\sum_{n=1}^{\infty}\frac{e^{-\sigma n}}{n^4} + 6\sigma\sum_{n=1}^{\infty}\frac{e^{-\sigma n}}{n^3} + \sigma^2\sum_{n=1}^{\infty}\frac{e^{-\sigma n}}{n^2}\right\} + \frac{8\bar{l}_1 + 6\bar{l}_2 + 5l_3}{12\pi^2\Sigma^2\gamma^4}T^3$$

$$\times\left\{6\sum_{m=1}^{\infty}\frac{e^{-\sigma m}}{m^2}\sum_{n=1}^{\infty}\frac{e^{-\sigma n}}{n^2} + 6\sigma\sum_{m=1}^{\infty}\frac{e^{-\sigma m}}{m}\sum_{n=1}^{\infty}\frac{e^{-\sigma n}}{n^2} + \sigma^2\sum_{m=1}^{\infty}\frac{e^{-\sigma m}}{m}\sum_{n=1}^{\infty}\frac{e^{-\sigma n}}{n} + \sigma^2(e^{\sigma}-1)^{-1}\sum_{n=1}^{\infty}\frac{e^{-\sigma n}}{n^2}\right\}$$

$$+ \frac{1}{2\Sigma^2\gamma^3}T^3\left\{12k(\sigma) - 6\sigma\frac{dk(\sigma)}{d\sigma} + \sigma^2\frac{d^2k(\sigma)}{d\sigma^2}\right\} + \mathcal{O}(p^8). \tag{D2}$$

In the above series, the spin-wave interaction manifests itself in the last two terms, which originate from two-loop and three-loop graphs. While the former involves the renormalized next-to-leading-order effective constants $\bar{l}_1$ and $\bar{l}_2$, the latter is proportional to the dimensionless function $k(\sigma)$ and its derivatives.

If we switch off the magnetic field, these low-temperature series turn into

$$u = \frac{\zeta(2)}{4\pi\gamma}T^2 + \frac{2l_3\zeta(3)}{\pi\Sigma\gamma^3}T^3 + \frac{9\left(4l_3^2 - c_1\Sigma\gamma\right)\zeta(4)}{\pi\Sigma^2\gamma^5}T^4 + \frac{5l_3\zeta(2)^2}{8\pi^2\Sigma^2\gamma^4}T^4 + \frac{k_0}{2\Sigma^2\gamma^3}T^4\left\{3\ln\left(\frac{\Lambda_p}{T}\right) - 1\right\} + \mathcal{O}(p^{10}),$$

$$s = \frac{\zeta(2)}{2\pi\gamma}T + \frac{3l_3\zeta(3)}{\pi\Sigma\gamma^3}T^2 + \frac{12\left(4l_3^2 - c_1\Sigma\gamma\right)\zeta(4)}{\pi\Sigma^2\gamma^5}T^3 + \frac{5l_3\zeta(2)^2}{6\pi^2\Sigma^2\gamma^4}T^3 + \frac{k_0}{2\Sigma^2\gamma^3}T^3\left\{4\ln\left(\frac{\Lambda_p}{T}\right) - 1\right\} + \mathcal{O}(p^8), \tag{D3}$$

$$c_V = \frac{\zeta(2)}{2\pi\gamma}T + \frac{6l_3\zeta(3)}{\pi\Sigma\gamma^3}T^2 + \frac{36\left(4l_3^2 - c_1\Sigma\gamma\right)\zeta(4)}{\pi\Sigma^2\gamma^5}T^3 + \frac{5l_3\zeta(2)^2}{2\pi^2\Sigma^2\gamma^4}T^3 + \frac{k_0}{2\Sigma^2\gamma^3}T^3\left\{12\ln\left(\frac{\Lambda_p}{T}\right) - 7\right\} + \mathcal{O}(p^8).$$

Again, the interaction part does not lead to a simple power of the temperature in the limit $H \to 0$; rather, it also involves a piece logarithmic in the temperature.

---

*christoph.peter.hofmann@gmail.com

[1] C. P. Hofmann, Phys. Rev. B **86**, 054409 (2012).

[2] F. J. Dyson, Phys. Rev. **102**, 1217 (1956); **102**, 1230 (1956).

[3] J. Zittartz, Z. Phys. **184**, 506 (1965).

[4] C. P. Hofmann, Phys. Rev. B **65**, 094430 (2002).

[5] C. P. Hofmann, Phys. Rev. B **84**, 064414 (2011).

[6] P. Gerber and H. Leutwyler, Nucl. Phys. B **321**, 387 (1989).

[7] C. P. Hofmann, Phys. Rev. B **60**, 406 (1999).

[8] S. Eggert, I. Affleck, and M. Takahashi, Phys. Rev. Lett. **73**, 332 (1994).

[9] O. A. Starykh, R. R. P. Singh, and A. W. Sandvik, Phys. Rev. Lett. **78**, 539 (1997).

[10] A. Klümper, Eur. Phys. J. B **5**, 677 (1998).

[11] W. McRae and O. P. Sushkov, Phys. Rev. B **58**, 62 (1998).

[12] C. Buragohain and S. Sachdev, Phys. Rev. B **59**, 9285 (1999).

[13] V. Yu. Irkhin and A. A. Katanin, Phys. Rev. B **61**, 6757 (2000).

[14] P. Hasenfratz and H. Leutwyler, Nucl. Phys. B **343**, 241 (1990).

[15] P. Hasenfratz and F. Niedermayer, Phys. Lett. B **268**, 231 (1991).

[16] P. Hasenfratz and F. Niedermayer, Z. Phys. B **92**, 91 (1993).

[17] H. Leutwyler, Phys. Rev. D **49**, 3033 (1994).

[18] C. P. Hofmann, Phys. Rev. B **60**, 388 (1999).

[19] J. M. Román and J. Soto, Int. J. Mod. Phys. B **13**, 755 (1999).

[20] J. M. Román and J. Soto, Ann. Phys. **273**, 37 (1999).

[21] J. M. Román and J. Soto, Phys. Rev. B **62**, 3300 (2000).

[22] C. P. Hofmann, AIP Conf. Proc. **623**, 305 (2002).

[23] C. P. Hofmann, Phys. Rev. B **81**, 014416 (2010).

[24] C. P. Hofmann, AIP Conf. Proc. **1361**, 257 (2011).

[25] C. P. Hofmann, J. Phys.: Conf. Ser. **287**, 012018 (2011).

[26] F. Kämpfer, M. Moser, and U.-J. Wiese, Nucl. Phys. B **729**, 317 (2005).

[27] C. Brügger, F. Kämpfer, M. Moser, M. Pepe, and U.-J. Wiese, Phys. Rev. B **74**, 224432 (2006).

[28] C. Brügger, F. Kämpfer, M. Pepe, and U.-J. Wiese, Eur. Phys. J. B **53**, 433 (2006).

[29] C. Brügger, C. P. Hofmann, F. Kämpfer, M. Pepe, and U.-J. Wiese, Phys. Rev. B **75**, 014421 (2007).

[30] C. Brügger, C. P. Hofmann, F. Kämpfer, M. Moser, M. Pepe, and U.-J. Wiese, Phys. Rev. B **75**, 214405 (2007).

[31] C. Brügger, C. P. Hofmann, F. Kämpfer, M. Moser, M. Pepe, and U.-J. Wiese, AIP Conf. Proc. **1116**, 356 (2008).

[32] F.-J. Jiang, F. Kämpfer, C. P. Hofmann, and U.-J. Wiese, Eur. Phys. J. B **69**, 473 (2009).

[33] F. Kämpfer, B. Bessire, M. Wirz, C. P. Hofmann, F.-J. Jiang, and U.-J. Wiese, Phys. Rev. B **85**, 075123 (2012).

[34] N. D. Vlasii, C. P. Hofmann, F.-J. Jiang, and U.-J. Wiese, Phys. Rev. B **86**, 155113 (2012).

[35] F.-J. Jiang, F. Kämpfer, B. Bessire, M. Wirz, C. P. Hofmann, and U.-J. Wiese, J. Phys.: Conf. Ser. **378**, 012034 (2012).

[36] U. Gerber, C. P. Hofmann, F. Kämpfer, and U.-J. Wiese, Phys. Rev. B **81**, 064414 (2010).

[37] U.-J. Wiese and H. P. Ying, Z. Phys. B **93**, 147 (1994).

[38] U. Gerber, C. P. Hofmann, F.-J. Jiang, M. Nyfeler, and U.-J. Wiese, J. Stat. Mech. Theory Exp. (2009) P03021.

[39] F.-J. Jiang and U.-J. Wiese, Phys. Rev. B **83**, 155120 (2011).

[40] U. Gerber, C. P. Hofmann, F.-J. Jiang, G. Palma, P. Stebler, and U.-J. Wiese, J. Stat. Mech. Theory Exp. (2011) P06002.

[41] C. P. Burgess, Phys. Rep. **330**, 193 (2000).

[42] T. Brauner, Symmetry **2**, 609 (2010).

[43] H. Leutwyler, in *Hadron Physics 94—Topics on the Structure and Interaction of Hadronic Systems*, edited by V. E. Herscovitz, C. A. Z. Vasconcellos, and E. Ferreira (World Scientific, Singapore, 1995), p. 1.

[44] S. Scherer, Adv. Nucl. Phys. **27**, 277 (2003).

[45] J. L. Goity, Czech. J. Phys. **51**, B35 (2001).

[46] S. Weinberg, Physica A **96**, 327 (1979).

[47] J. Gasser and H. Leutwyler, Ann. Phys. (NY) **158**, 142 (1984); Nucl. Phys. B **250**, 465 (1985).

[48] H. Leutwyler, Ann. Phys. (NY) **235**, 165 (1994).

[49] V. Mubayi and R. V. Lange, Phys. Rev. **178**, 882 (1969).

[50] J. H. P. Colpa, Physica **57**, 347 (1972).

[51] K. Yamaji and J. Kondo, Phys. Lett. A **45**, 317 (1973).

[52] M. Takahashi, Prog. Theor. Phys. Suppl. **87**, 233 (1986).

[53] M. Takahashi, Phys. Rev. Lett. **58**, 168 (1987).

[54] M. Takahashi, Jpn. J. Appl. Phys. Suppl. **26**(3), 869 (1987).

[55] M. Takahashi, Prog. Theor. Phys. **83**, 815 (1990).

[56] A. Auerbach and D. P. Arovas, in *Field Theories in Condensed Matter Physics*, edited by Z. Tesanovich (Addison-Wesley, Reading, MA, 1990), p. 1.

[57] F. Suzuki, N. Shibata, and C. Ishii, J. Phys. Soc. Jpn. **63**, 1539 (1994).

[58] H. Nakano and M. Takahashi, Phys. Rev. B **50**, 10331 (1994).

[59] D. A. Yablonskiy, Phys. Rev. B **44**, 4467 (1991).

[60] M. Kollar, I. Spremo, and P. Kopietz, Phys. Rev. B **67**, 104427 (2003).

[61] N. D. Mermin and H. Wagner, Phys. Rev. Lett. **17**, 1133 (1966).

[62] G. Leibbrandt, Rev. Mod. Phys. **47**, 849 (1975).

[63] P. Kopietz and S. Chakravarty, Phys. Rev. B **40**, 4858 (1989).